Available online at www.sciencedirect.com
ScienceDirect
Forest Ecology and Management 248 (2007) 95–106
Forest Ecology and Management
www.elsevier.com/locate/foreco

Simulating the extent of decay caused by *Heterobasidion annosum s. l.* in stems of Norway spruce

Thomas Seifert *

Technische Universität München, Am Hochanger 13, 85354 Freising, Germany

Accepted 8 February 2007

Abstract

Heterobasidion annosum (FR.) BREF. sensu lato causes severe economic damage in stands of Norway spruce (*Picea abies* [L.] Karst). The primary damage is the deterioration of timber by decay. Secondary damage can be attributed to higher risks of windthrow and stem breakage, growth reduction of infected trees as well as higher machining and handling costs for decayed stems during grading and processing. Regardless of the importance of this pathogen there are very few software tools which support management decisions in red rot affected forests and none of them are parameterised with data from Central Europe.

The present study aimed to develop a model which is able to spatially predict the extent and degree of decay in the stem as well as its effects on the growth of Norway spruce. This involves the integration of several sub-models into a tree growth simulator: (i) diameter of decay, (ii) height of decay, (iii) form of decay, (iv) degree of decay, and (v) feedback of the pathogen on tree growth. The model is parameterised mainly from published data of other authors. The input for the time of infection of a tree is delivered from a separate model. A grading algorithm is used to evaluate the impact of different scenarios on the revenue of infected stands in typical stands of Norway spruce in Germany. This integrated system of growth and red rot simulation is able to support management decisions on various levels and documents that if red rot is not taken into consideration in the affected stands, clear misinterpretations and thus inaccuracies will arise in the economic results from tree growth simulators. The need for further research was identified especially in model validation and the tree–pathogen interaction.

Keywords: *Heterobasidion annosum*; *Picea abies*; Stem decay; Rot model; Growth simulation; Wood quality

1. Introduction

Annosum root rot caused by the wood decaying basidiomycetous fungus *Heterobasidion annosum* [FR.] BREF. accounts for severe financial losses in forestry, e.g. within stands of Norway spruce (*Picea abies* [L.] Karst). In this publication *H. annosum* is referred to in sensu lato because most of the cited older publications which include the ones used for the model development do not distinguish between the different species of *Heterobasidion*.

H. annosum is able to infect a tree either by spores through wounds in the bark and the root collar or by intrusion via the roots from infected neighbouring trees and stumps. These two ways of infection may involve a distinct difference in pathogenesis (von Pechmann and von Aufsess, 1971; von Pechmann et al., 1973; Binder, 1995). Typically the fungus spreads via spores, which colonize freshly cut stumps creating an effective platform for the fungus to spread to living trees over the root system (Stenlid and Redfern, 1998). In contrast, *H. annosum* is often outcompeted by other species in the colonization of stem wounds (Isomäki and Kallio, 1974).

The damage caused by this pathogen is manifold. Most obvious of all is the deterioration of the timber by stem decay, a white rot where lignin is degraded. The damage is especially high because the most valuable butt log is decayed, which in turn limits the timber use for aesthetical and mechanical purposes. As a result, the attainable timber prices are reduced (Seifert, 2003). Schumacher et al. (1997) identified stem rot in grading trials of Norway spruce logs according the European grading rule EN1927-1 to be the most important grading variable together with branchiness.

There is also a risk of severe collateral damage as decayed trees obviously have higher probabilities of being thrown or broken by storms or snow (Bazzigher and Schmid, 1969;

* Tel.: +49 8161 714 713; fax: +49 8161 714 721.
E-mail address: seifert@lrz.tum.de.

0378-1127/$ – see front matter © 2007 Elsevier B.V. All rights reserved.
doi:10.1016/j.foreco.2007.02.036

Dimitri and Tomiczek, 1998; Steyrer and Tomiczek, 1998) and require more time- and cost-consuming handling in the grading and bucking process (Kató, 1969; Johann, 1988). Additionally, there are strong indications that the growth of infected trees is reduced (Henriksen and Jørgensen, 1952; Arvidson, 1954; Kallio and Tamminen, 1974; Bendz-Hellgren and Stenlid, 1995, 1997). Seifert (2003) provided a comprehensive review on the different economic and ecologic impacts of the fungus. An estimated annual loss of €790 million for the area of the European Union in 1998 (Woodward et al., 1998) may even be an underestimation.

The obvious economic relevance and the serious ecologic impact of the pathogen on stand stability forced early botanists and forest scientists to deal with the biology of the pathogen.

Since Theodor and Robert Hartig identified the aetiology of the pathogen and recognized its importance for forestry mainly in the early 19th century (Hüttermann and Woodward, 1998), much research has been conducted on this pathogen. In the last century, centres of research were established in the United Kingdom, Scandinavia, and Central Europe which had the objective to reveal the processes of pathogenesis as well as to empirically quantify the relationships between tree dimension and decay. The latter research line produced many relevant findings and is the basis for further quantitative estimation of losses by *H. annosum*. Important authors to mention in this context are, for example, Arvidson (1954), Kató (1967), Zycha (1967a,b), Zycha et al. (1970), Werner (1971), Rehfuess (1969, 1973), von Pechmann et al. (1973), Kallio and Tamminen (1974), Pratt (1979), Dimitri (1980), Johann (1988).

The ambitions of the current researchers deal with the transformation of the present expertise in simulation models to describe the spread of the pathogen throughout the stand (Frankel et al., 1994; Vollbrecht and Jørgensen, 1995; Pratt et al., 1998; Möykkynen et al., 1998, 2000; Müller, 2002; Pukkala et al., 2005) with the objective to calculate losses and adequate treatment scenarios. The combination of the simulation models with existing forest growth models was a necessary step to support the decisions made on the forest management level.

There are some flaws, however, in the existing models. Most of them are parameterised for Scandinavia and it is not clear whether they can be assigned to conditions in Central Europe. The only approach which attempts to integrate growth simulators all over Europe is the transnational MOHIEF-framework (Woodward et al., 2003). However a second shortcoming of this and most other models is that they concentrate on the spread of the pathogen in the stand from tree to tree and lack a proper description of the decay in the stem. The existing approaches mostly approximate decay dimension and form in the stem very roughly by cones (Möykkynen et al., 2000; Pukkala et al., 2005) or other geometric primitives and neglect the specific pathogen–tree interaction.

Since an adequate spatial description of the decay is a necessary prerequisite for an optimised grading according to timber quality and virtual sawing, a model named 'RAM' was developed which is able to make plausible predictions of the dimension, form and degree of decay in the stem of Norway spruce under central European conditions (Seifert, 2003). The model is focussed on the simulation of heart rot originating from an infection over the root system. An important aspect of the model is the tree–pathogen interaction which is able to reflect different developments of decay depending on stand management and site conditions. These objectives involve the integration of the rot models in a forest growth simulator. In this work the distance dependent single tree simulator SILVA (Pretzsch et al., 2002a) with the integrated red rot infection model RIM (Müller, 2002) is used. The newly developed model should be able to interact with the cited models to form a model framework to support management strategies for stands infected with *H. annosum* in the future.

2. Data base

The sub-models of RAM are based on published data of other authors. The data originate mainly from Central Europe with a focus on Germany. An exception is the data on pathogen induced growth reduction after infection, which were only available from Scandinavian stands. The data base of the models is illustrated in Table 1. Most of the data were gathered in the scope of a joint research programme of the German Research Agency (DFG) during the 1960s and 1970s. During the modelling process, data from different studies were combined and statistically re-evaluated. This involved data retrieval from published graphs since only a part of the data was published in tabular format. In most instances no data were published at tree level. Only average values and variances at stand level were available.

Table 1
The data base of the model RAM consists of the published work of many authors which was partly re-analysed

Sub-model	Author	Region	No of trees	No of stands
RD, RRA	von Pechmann et al. (1973)	Bayern	863	9
	Rehfuess (1969, 1973)	Baden-Württemberg	860	20
	Zycha (1967a,b)	Nordrhein-Westfalen, Niedersachsen, Hessen	1877	39
RH_{max}	Zycha et al. (1970)	Nordrhein-Westfalen, Niedersachsen, Hessen	956	17
	von Pechmann et al. (1973)	Bayern	863	9
*i*RH	Synthesis of diverse publications (Seifert, 2003)	Germany, United Kingdom, Scandinavia		
DD	Kató (1967)	Niedersachsen	230	–
ΔBHD, Δ*H*	Bendz-Hellgren and Stenlid (1997)	Sweden	68	National forest inventory

3. Model specification

3.1. Rationale of the model 'RAM'

A foundation of the model is the assumption that there are two phases of development in the decay inside the stem. In the first phase (*phase A*) the fungus decays only heart wood when it enters the stem from the coarse roots. As there is no interaction with living cells of the tree, the fungus develops more or less independently. After the fungus reaches the sapwood–heartwood boundary, the second phase (*phase B*) is initiated. This phase is characterised by a close tree–pathogen interaction. In a constant battle at the border of the sapwood, the fungus tries to invade the sapwood while the tree tries to defend itself by inducing chemical and mechanical barriers (von Weissenberg, 1998; Asiegbu et al., 1998). It is here that the so called reaction zone is formed (Shain, 1971; Haars et al., 1981; Stenlid and Redfern, 1998). The defence, in combination with the low oxygen content of the sapwood, effectively prevents the fungus from the oxidative degradation of sapwood (Courtois, 1970; Cwielong et al., 1993). The fungus can only grow further if new heartwood is formed. For that reason the development of decay is restricted and it very much depends on tree growth. In return, also tree growth is influenced by the fungus due to a trade-off to defence which cannot be invested in primary growth.

3.2. Prediction of decay diameter at stem base

The prediction of the diameter of decay at the base of the stem is based on the assumption that the ratio of decay area to the stem cross sectional area, both measured at stem base, is more or less constant for all trees in one stand. This is supported by findings of Zycha and Dimitri (1968), Zycha et al. (1970), and von Pechmann et al. (1973) and seems to be valid for mature stands, where the fungus was already established. The described ratio is called 'relative rot area' (RRA) further on. The relative rot area seems to be independent of the social status of a tree (von Pechmann et al., 1973). Zycha (1967b) concludes from his findings that a faster tree growth is compensated by higher rot areas.

Except for the fact that young spruce trees were not susceptible to *H. annosum* attacks (Dimitri, 1980; Bazzigher, 1986; Rieger, 1991) tree age had no influence on RRA but site conditions seemed to have an influence (Zycha and Ulrich, 1969; Zycha, 1967a; Rehfuess, 1969, 1973; von Pechmann et al., 1973; Seifert, 2003). In this context it is important to mention that all the finally quoted studies were analysing mature stands where we can assume a tree–pathogen interaction in phase B and not in an initial phase.

To account for site specific relative decay diameters and areas the prediction of RRA was chosen as an input variable which has to be determined by the user. From experience or probing during a felling or thinning the RRA can be estimated easily. The input in the model is conducted with an average value for the RRA and a typical standard deviation.

Within the simulation a specific RRA for each infected tree is estimated by means of a stochastic process based on the average $\bar{x}$ and the variance σ^2 to reproduce the observed variance in the data. A random number generator is used to generate RRA values which distribute normally with $N(\bar{x}\sigma^2)$. The resulting tree specific RRA is used to determine the maximum rot diameter like it will be in phase B according to Eq. (1)

$$\mathrm{RD}_{\max} = \left(\frac{\mathrm{RRA}}{100} \times D^2\right)^{1/2} \tag{1}$$

with $\mathrm{RD}_{\max}$ being the maximum rot diameter at stem base [cm], RRA the relative rot area and D is the stem diameter at stem base [cm]. D is calculated for each tree by the growth simulator according to the stem taper model BDAT (Kublin and Scharnagl, 1988) which is integrated in the growth simulator SILVA. To account for the initial expansion of decay in the heartwood (phase A) a proportionality of the height and the diameter growth of the fungus is presumed. The initial rot diameters are calculated according to Eq. (2).

$$\mathrm{RD}_t = \frac{\mathrm{RD}_{\max}}{\mathrm{RH}_{\max}} \times \mathrm{RH}_t \tag{2}$$

with RD_t and RH_t being the rot diameter at stem base and the rot height, respectively. At time t, $\mathrm{RH}_{\max}$ is defined as the maximum rot height in phase B [cm]. With Eqs. (1) and (2) it is possible to predict a rapid unrestricted radial expansion of the decay, which is more or less independent of tree growth (phase A). If the maximum growth of the rot is reached the radial spread of decay slows down and is restricted by the development of the heartwood (phase B). $\mathrm{RD}_{\max}$ can bee understood as a substitute for the heartwood size.

3.3. Prediction of decay height

For the height prediction the same phase concept was applied. The initial rot height increment is assumed to be an empirically determined constant in phase A and the actual rot height is assumed to be a function of time from infection (Eq. (3)).

$$\mathrm{RH}_t = \mathrm{TI} \times i\mathrm{RH} \tag{3}$$

with RH_t being the rot height at a certain date in phase A [cm], TI being the time since intrusion of the stem [years] and iRH the yearly height increment of the decay [cm].

For the prediction of rot height in the phase B a regression model was fitted to the existing data based on the least squares method with the RRA as the main predictor (Eq. (4)).

$$\mathrm{RH}_{\max 1} = b1 \times D + b2 \times \mathrm{RRA} \quad \text{for } 15 \leq \mathrm{RRA} \tag{4}$$

with $\mathrm{RH}_{\max\ 1}$ being the maximum rot height in phase B [cm], D being the stem diameter at stem base [cm], RRA being the relative rot area at stem base [%], and $b1$ and $b2$ being regression parameters (Table 2). The parameterisation of the model was based on the combination of data from different authors (Table 1). The stem diameter was incorporated additionally because it showed a significant additional effect on the height of the rot after the combination of the data. Since no data was available for a RRA smaller than 15, and no nonlinear model gave a better fit than the linear model in the range of parameter-

Table 2
Acronyms and model parameters given in the text

Variable/ parameter	Unit	Description	Parameter value
D	cm	Diameter at stem base	
DD		Degree of decay	
DD_I		Degree of decay I	
DD_{III}		Degree of decay III	
iRH	cm	Yearly rot height increment in phase A	30
RD	cm	Total diameter of decay at stem base (=RD_I)	
RD_{III}	cm	Diameter of the decay with a DD_{III}	
RD_{max}	cm	Maximum rot diameter at stem base	
RD_t	cm	Rot diameter at stem base at time t	
RH	cm	Total height of decay (=RH_I)	
RH_{III}	cm	Height of the decay with DD_{III}	
RH_{max}	cm	Maximum rot height	
RH_t	cm	Rot height at stem base at time t	
RRA		Proportion of rot area to total stem area at stem base	
TD_{dep}	Years	Time since beginning of diameter depression	
TH_{dep}	Years	Time since beginning of height depression	
TI	Years	Time since invasion of the decay in the stem	
ΔBHD	%	Relative diameter depression	
ΔH	%	Relative height depression	
ΔiBHD	%	Relative diameter increment depression	
ΔiH	%	Relative height increment depression	
$b1$		Regression parameter Eqs. (4) and (5)	4.1640
$b2$		Regression parameter Eqs. (4) and (5)	10.4290
$d1$		Regression parameter Eq. (9)	0.4520
$d2$		Regression parameter Eq. (9)	−0.2231
$e1$		Regression parameter Eq. (10)	0.1810
$e2$		Regression parameter Eq. (10)	−0.0487
$f1$		Regression parameter Eq. (11)	−0.4462
$g1$		Regression parameter Eq. (12)	−0.0974

isation, a segmented linear model was constructed with Eq. (4) representing the second segment. With regard to the first segment, the simulation of RRA smaller than 15 should fit to the parameterised Eq. (4) without gap. The resulting formulation is shown in Eq. (5).

$$RH_{max\,2} = \frac{(b1 \times D)}{15 + b2} \times RRA \quad \text{for } 0 \leq RRA \leq 15 \tag{5}$$

For relative rot area ratio beyond 45 the linear regression of Eq. (4) is assumed to be valid.

In Fig. 1 the model fit is shown. In Fig. 2 the sensitivity of the model to stem diameter changes is displayed and a comparison with a linear approach proposed by von Pechmann et al. (1973).

3.4. Prediction of the degree of decay

Following Zycha (1962), red rot can be visually classified in four discrete levels of degree of decay—DD_I: discoloration, no structural decay; DD_{II}: beginning structural decay, timber still sawable; DD_{III}: severe structural decay, but structure maintains, not sawable; DD_{IV}: total collapse of the wood structure. The most severe changes on wood quality are the transition from

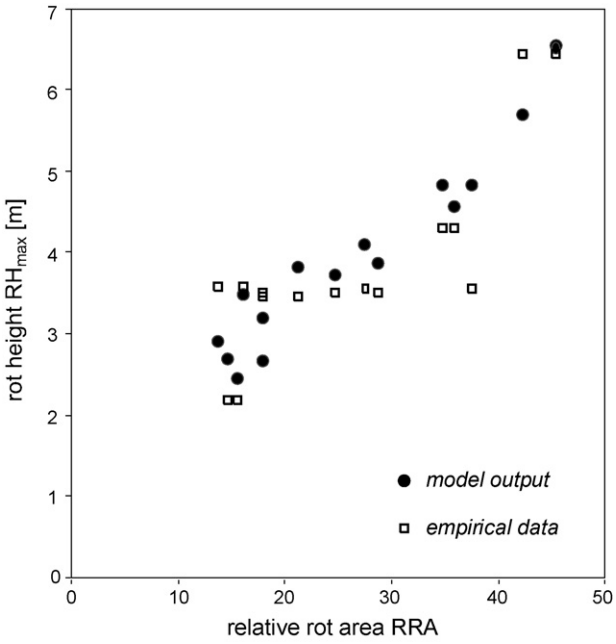

Fig. 1. Fit of the model to predict height of the decay in the stem.

DD_{II} to DD_{III}. Most of the studies cited in Table 1 adopt Zycha's classification scheme.

We simulate the degree of decay as a function of rot diameter according the results of Kató (1967). The original function of Kató was transformed from the continuous to a discrete form with the classification according to the defined four decay classes. Once a predicted rot diameter has reached a certain threshold the next, more severe level of decay is assigned and attributed to the middle of the disc (Eq. (6)). This results in concentric rings of different decay level with the higher levels in the centre of the stem.

$$DD = \begin{cases} \text{I for RD in } < 11.02\,\text{cm} \\ \text{II for RD in } [11.02 - 27.04]\,\text{cm} \\ \text{III for RD in }]27.04 - 51.11]\,\text{cm} \\ \text{IV for RD in } > 51.11\,\text{cm} \end{cases} \tag{6}$$

with DD being the degree of decay according to Zycha (1962) and RD being the rot diameter at stem base.

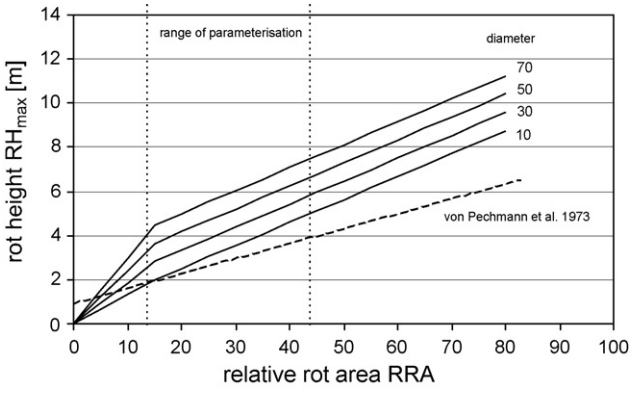

Fig. 2. Sensitivity of the rot height model to stem diameter and comparison with a linear model proposed by von Pechmann et al. (1973).

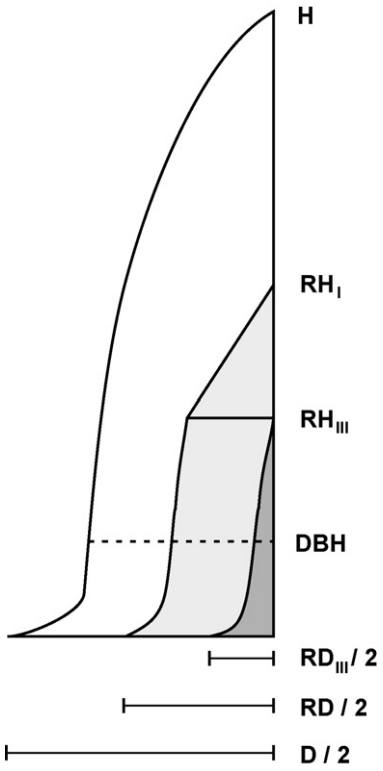

Fig. 3. Geometrical shape of the rot form model in RAM. *H*: tree height; RH: height of the total rot; RH_{III}, RD_{III}: height, diameter respectively of the part of the rot which is of degree III; DBH: diameter in breast height; RD and *D*: diameter of the decay and the stem respectively at stem base.

3.5. Prediction of decay form

The rot form can be described as the change of rot diameter along the height of the decay column. The rot form model implies a centric rot form which can be assumed for the majority of the decayed trees (Werner, 1971; Graber, 1996).

In the implemented simulation model, rot form results from the previous models with some additional assumptions. These account for the form changes of different parts of the decay column with specific degrees of decay. For this reason it is modelled in close relation with the other models. In Fig. 3 the geometrical shape of the form model is illustrated.

Zycha and Dimitri (1968) stated that rot form equals stem form if the degree of decay at stem base is at level III or IV. For the simulation, first the degree of decay at stem base is checked according to Eq. (6). If a degree of decay of III or more is predicted, the part of the decay with DD_{III} could be determined for any defined height according to Eq. (7) which follows from Eq. (6).

$$RD_{III} = RD - 27.04 \tag{7}$$

with RD_{III} being the diameter of the share of the decay cross section which has a degree of decay of III or more [cm] and RD being the total diameter of the decay at stem base [cm].

In the following step the height of the decay column featuring a DD_{III} or more is calculated. A proportional height diameter development is assumed (Eq. (8)).

$$RH_{III} = \frac{RD_{III}}{RD} \times RH \tag{8}$$

with RH_{III} being the height of the share of the decay cross section which has a degree of decay of III or more [cm] and RH being the total height of the rot [cm].

Rot form of degree I is modelled so that it follows the former stem form which is delivered from the stem taper model used in the growth simulator SILVA (Fig. 3).

If the estimated RD_I is lying between 2 year rings, the outermost ring is the one which is used. The rot form of degree II and III and IV are determined by subtracting the thresholds defined in Eq. (6) from the estimated form of degree I. This approach assures a dynamic interaction of rot expansion with stem growth as presumed for phase B. Above RH_{III} the rot development is simulated by a cone because no interaction with the tree growth occurs in phase A.

3.6. Prediction of growth reduction of infected trees

No data from Central Europe was available for the growth reduction of trees in the course of stem decay. For this reason, Scandinavian data was used to identify the relative height and diameter growth loss of trees which had an apparent rot at stem base (Table 1). This can be done providing that trees suffer from the same relative growth losses irrespective of their size, the site and climate conditions.

The data of Bendz-Hellgren and Stenlid (1997) were retrieved from the published graphs. Regression fitting with the least squares method proved that non-linear models were more suitable than linear models to describe the reduced growth as a function of time elapsed since the depression started (Figs. 4 and 5).

For this reason Eqs. (9) and (10) were established with a quadratic polynomial fit to account for the nonlinear development of reduced growth.

$$\Delta H = d2 \times TH_{dep}^2 + d1 \times TH_{dep} \tag{9}$$

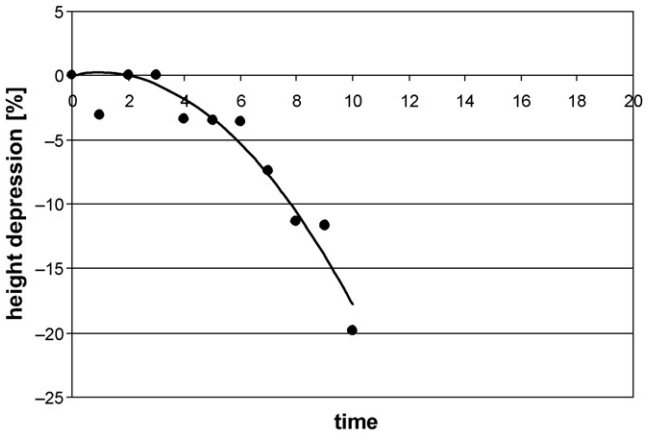

Fig. 4. Height depression since intrusion of the decay in the stem modelled with a quadratic polynomial.

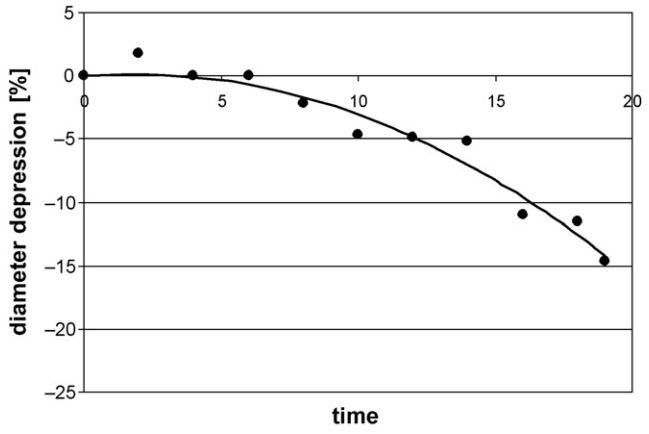

Fig. 5. Diameter depression since intrusion of the decay in the stem modelled with a quadratic polynomial.

$$\Delta\mathrm{BHD} = e2 \times \mathrm{TD}_{\mathrm{dep}}^2 + e1 \times \mathrm{TD}_{\mathrm{dep}} \quad (10)$$

with ΔH and ΔBHD being the relative loss in growth after a certain time span in percent compared to non-infected trees, $\mathrm{TH}_{\mathrm{dep}}$ and $\mathrm{TD}_{\mathrm{dep}}$ being the time elapsed since the start of the height and diameter growth reduction (we can assume that this is the time when the sapwood is challenged by the fungus, that means with the beginning of $\mathrm{DD}_{\mathrm{III}}$). The parameters are summarized in Table 2.

Due to the fact that a yearly increment loss was to be included in the growth simulator rather than a summed growth loss, Eqs. (9) and (10) were differentiated which lead to Eqs. (11) and (12).

$$\Delta iH = f1 \times \mathrm{TH}_{\mathrm{dep}} + d1 \quad (11)$$

$$\Delta iD = g1 \times \mathrm{TD}_{\mathrm{dep}} + e1 \quad (12)$$

with ΔiH and ΔiD being the yearly reduction in height and diameter increment [%]. Parameters are given in Table 2.

With the integration of the proposed models in the growth simulator, a feedback of decay on tree growth can be simulated. To ensure a logical model behaviour the predicted values of Eqs. (11) and (12) are set to a constant for 100% growth reduction (no increment) if the model would predict more than 100% to avoid that the predicted growth reductions exceed logical boundaries. This is the case after 225 and 1028 years for the height and the diameter model, respectively. However, in none of the scenario simulations such a long period was simulated.

4. Simulation results

4.1. Simulation of tree growth and spread of the fungus in the stand

As mentioned the models for decay prediction in the stem were integrated in the growth simulator SILVA (Pretzsch, 2002; Pretzsch et al., 2002a) which serves as a framework for all sub-models. SILVA is a single tree simulator which predicts tree growth depending on site factors and the spatial positioning of the tree in the stand. It represents an empirical approach for growth estimation and is parameterised for several countries in Central Europe. SILVA is able to import inventory data and provides a wide range of silvicultural management options as well as a wood quality sensitive grading and bucking routine which is based on optimisation with a genetic algorithm (Seifert, 2003). SILVA was evaluated according the standards defined by Pretzsch et al. (2002b). The infection probability and the time of infection is modelled tree wise by the model RIM (Müller, 2002) which is also part of SILVA. With this stochastic approach it is possible to predict a plausible spread of the fungus by spores and by roots from tree to tree because the spatial tree distribution and dimension are explicitly modelled. The basic concept of RIM is the combination of stochastic models with spatial elements. The first stochastic probability is the occurrence of spores in the stand. The second probability accounts for the chance that a tree or a stump is infected by spores. The third probability is the one to have a successful infestation of the fungus. The fourth probability describes the chance of a secondary root to root infection by an already infected tree or a stump. This model provides the spatial component of RIM because it takes into account tree dimensions as well as tree position. The overlapping areas of the root systems of a non-infected and an infected tree is the main factor which modifies the probability of a successful propagation from root-to root. This fourth probability, which is additionally modified by soil acidity, also decides over the fact whether a tree can successfully defend itself against an attack. When a tree defended itself against the fungus it is defined to be immune to future attacks. A separate model calculates the spread inside the root system because an infection of another tree only takes place under the assumption that the fungus reaches the stump and invades other roots from there. Another model provides information on the spatial decline of the root system of a stump after the tree was felled. Typical growth rates in the roots and all other stochastic parameters of RIM are derived from literature (Müller, 2002).

4.2. Scenario set up

To test the plausibility of the combined simulation of all sub-models, two scenarios were calculated. Scenario A is based on a stand of pure Norway spruce with an initial age of 18 years with 1950 trees per hectare. The growth was projected up to an age of 128 years for a site in southern Germany on a site with good water and nutrient supplies and which is typically subject to red rot. A conservative thinning from below was applied in 5 years intervals. The infection rates in the stand over time simulated by SILVA and RIM are shown in Fig. 6.

The trees in the stand were assumed to have a heavy decay like those of stands derived from afforestation on former arable land. Subsequently 60% of average RRA was defined as a model input with a standard deviation of 15%. For the stand level interpretation the scenario run was repeated 10 times to avoid a bias due to stochastic components of SILVA, RIM, and RAM. The scenario is used to exemplify the decay of timber in

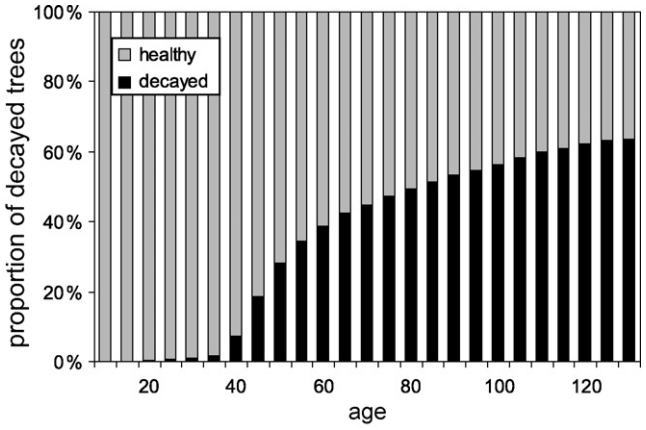

Fig. 6. Scenario showing the infection rates of trees in the simulated stand estimated by the epidemiologic model RIM (Müller, 2002).

the single tree and the whole stand. A third aspect is the simulation of feedback of decay on tree growth.

Scenario B is more focussed on assortment and economic yield since it makes use of the grading and sorting model SILVSORT (Seifert, 2003) in SILVA which is sensitive to wood quality and calculates an optimal bucking pattern on the tree level by means of a genetic algorithm.

The growth of a stand of Norway spruce was simulated for 40 years, starting at age 63 until the time of harvest at age 113. Stem number was reduced from 669 to 466 per hectare by a moderate thinning from below, which lead to a basal area increase from 53 to 73 m^2 per hectare. A typical moderate RRA of 35 is assumed with a standard deviation of 10.

4.3. Scenario A: simulation results at single tree level

The results of the model RAM is exemplified over simulation time for a heavily decayed tree in Fig. 7. For the sake of clarity, only the rot form of level I and level III are displayed.

It is obvious that at 68 years of age there is only a very small amount of decay, which is growing independently of stem

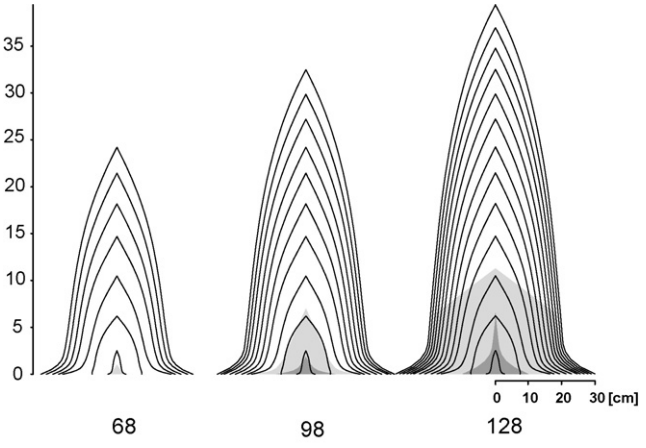

Fig. 7. Chronological development of the extent of decay in a simulated Norway spruce stem. The illustration shows the discoloured (light grey) and the heavily decayed (darker grey) rot zone as well as the stem taper in 10 years intervals.

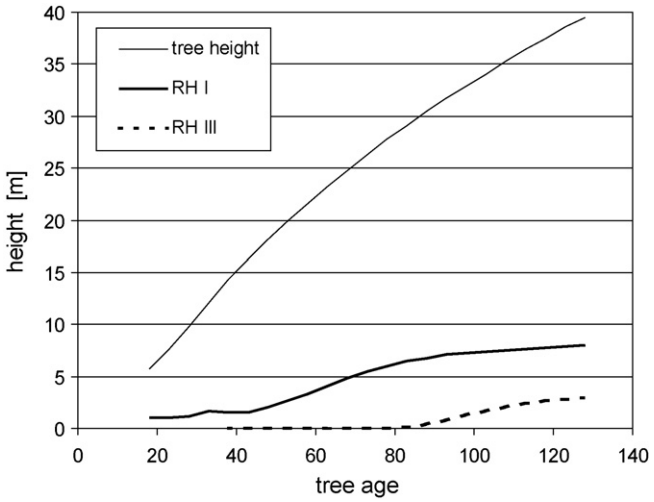

Fig. 8. Simulated height development of decay of degree I (discolouration) and degree III (not sawable).

growth and is therefore predicted by a cone (phase A). When the tree grows older and reaches an age of 98 (a typical harvesting age for Norway spruce at these sites) the decay of level I (discoloration zone) has expanded to a height 7 m, while also the level III decay was formed and reached an axial extent of 2.1 m. Consequently, the level I rot form followed the former stem development in the lower part of the stem (phase B) while at the upper part of the stem the rot still grew like a cone (phase A). At an age of 128 the discoloration zone exceeds the 11 m and has covered most of the stem cross section. The heavily decayed zone, with a decay class of III, has reached up to nearly 7 m. Again the results reflect the two phases of the tree–pathogen interaction. The dimensions of rot compare well to the maximum values of Kató (1967) or Werner (1971).

4.4. Scenario A: simulation results at stand level

The results at stand level (Figs. 8 and 9) show the development of the stem and rot height plus the stem

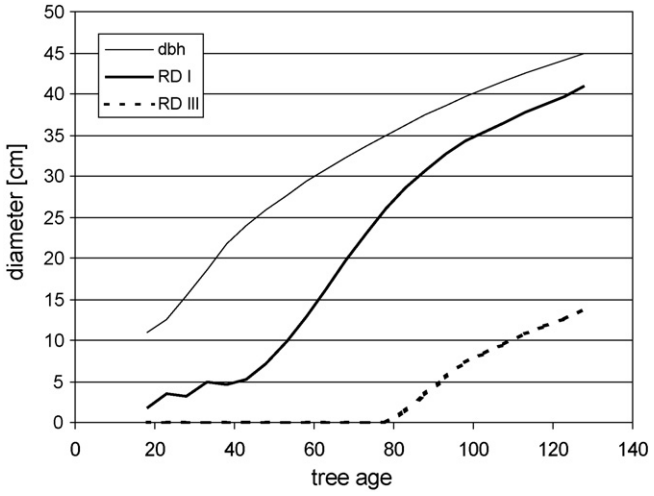

Fig. 9. Simulated diameter development of decay of degree I (discolouration) and degree III (not sawable).

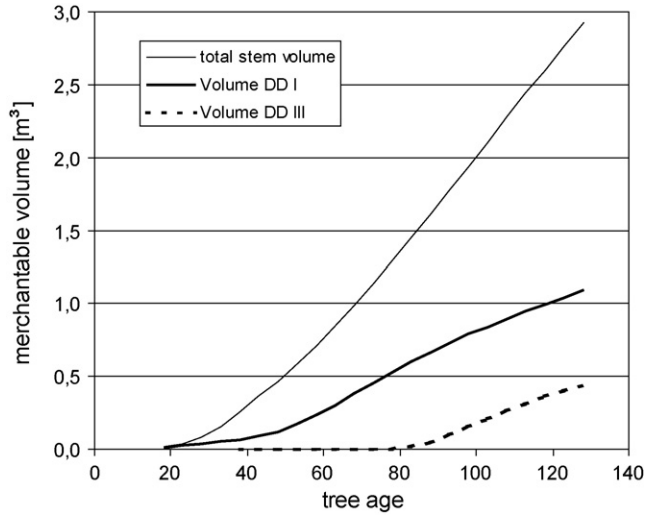

Fig. 10. Simulated stem volume which is affected by decay of degree I (discolouration) and degree III (not sawable).

and rot diameter for an average tree in the stand. Only the infected trees were considered. In Fig. 10 the volume development of the stem and the decay are illustrated.

The results for decay differentiate between discoloured (DD_I) and heavily decayed (DD_{III}) parts of the rot. It is obvious that decay of level III is not developing before an age of 60 years in this simulation. Furthermore, it is clear that the height expansion of the decay compared to the tree height extension is considerably slower than the ratio of radial rot extension to stem diameter. In Fig. 8 the effect on the merchantable volume is shown. The chosen scenario predicts a faster development of stem volume than of decay volume. Nonetheless, the most valuable parts of the butt end of the stem are deteriorated.

4.5. Scenario A: feedback on tree growth

Growth reduction is attributed to all trees where the rot at stem base is at least of degree of decay III. The simulation revealed that due to the bigger root systems larger trees had also a higher probability to get infected. This confines well with the findings of Pukkala et al. (2005). It is a well known fact that the dominant trees of a stand have higher growth increment (see e.g. Wipfler et al., 2005). For this reason the diameter has to be taken into account to compare the growth increment of infected and healthy trees in the stand. To avoid a bias on the interpretation of results a comparison of pairs of infected and

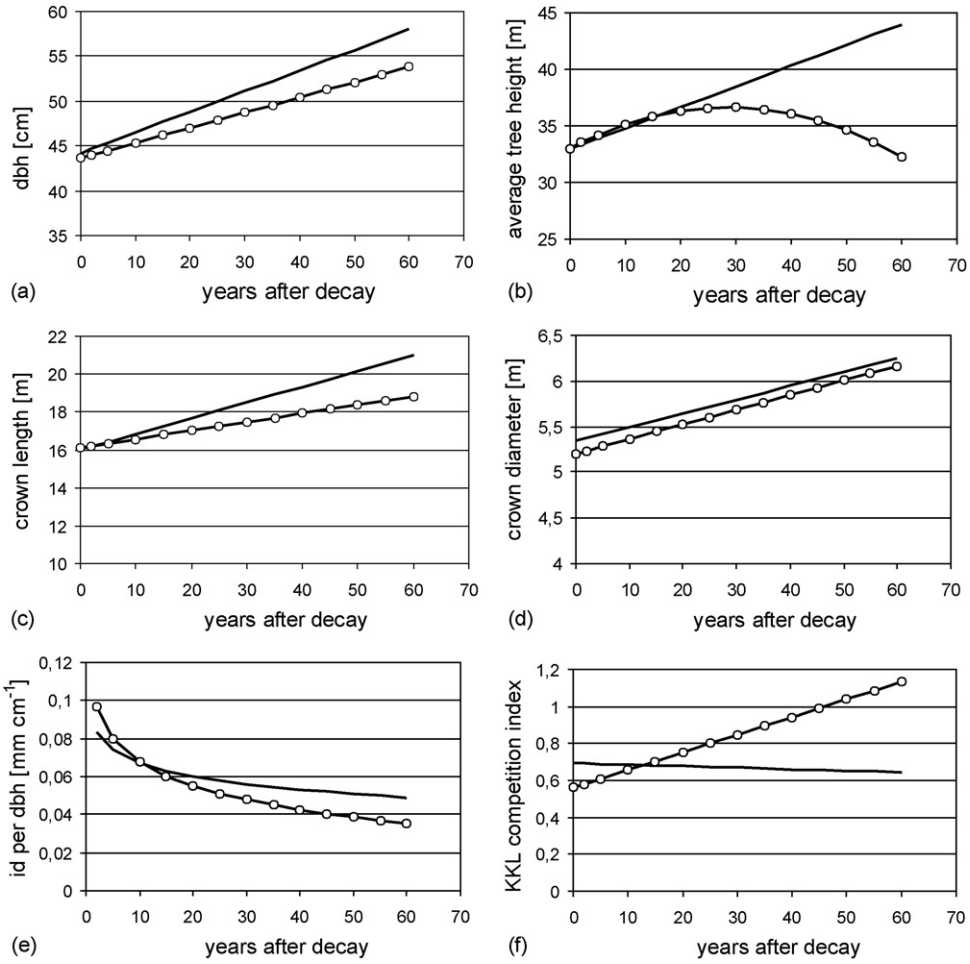

Fig. 11. Results of simulation scenario A: feedback of the fungus on tree growth. The growth and growing situation of infected (pointed line) and healthy trees (solid line) are compared: (a) diameter, (b) height, (c) crown length, (d) crown diameter, (e) diameter increment per stem diameter in the preceding period, (f) competition index 'KKL' (refer to text).

healthy trees was performed. Only trees with a similar diameter (tolerance ± 0.5 mm) and height (tolerance ± 1.0 m) were compared. Furthermore the average diameter growth of the last 15 years before infection was compared to select 148 pairs in the end.

The decayed trees showed a reduction in diameter and especially height growth (Fig. 11a and b). Their crown length was clearly reduced while crown diameter showed no strong effect (Fig. 11c and d). Altogether they lost crown volume and competitive strength which decreased their diameter increment per diameter, measured in the preceding period compared to healthy trees (Fig. 11e). This fact is also illustrated by a competition index in Fig. 11f. An index called KKL (Pretzsch et al., 2002a) was calculated to account for the spatial size relation to the competitors around. The decayed trees had less competition at the beginning than the healthy. During ongoing decay the decayed trees suffered from increasing competition. The healthy trees in contrast showed a slight decrease of competition. While the decayed trees lost social status due to their reduced growth rate, the healthy trees seemed to profit from the available space.

4.6. Scenario B: consequences for assortment and economic yield

The second scenario is calculated to clarify the effects of red rot on the assortment structure and the economic return. In Fig. 12 the results of the sorting are displayed.

The results show an optimal bucking and grading pattern for the simulated stand based on defined price and cost assumptions. The grading is done according to the European grading norm EN1927-1. When red rot is taken into account the assortments shift obviously from the better classes (B) to the worse ones (C) like illustrated in Fig. 12. Also the amount of small sized chipping wood IL N increased when decay was considered in the grading simulation.

The effects on revenue are obvious. If the grading and bucking of the simulated logs was performed sensitive to decay the net revenue of the timber was €43,820 per hectare after subtracting harvesting costs. If decay was not considered the net revenue was predicted to be €64,760. This equals an overestimation of nearly 48%.

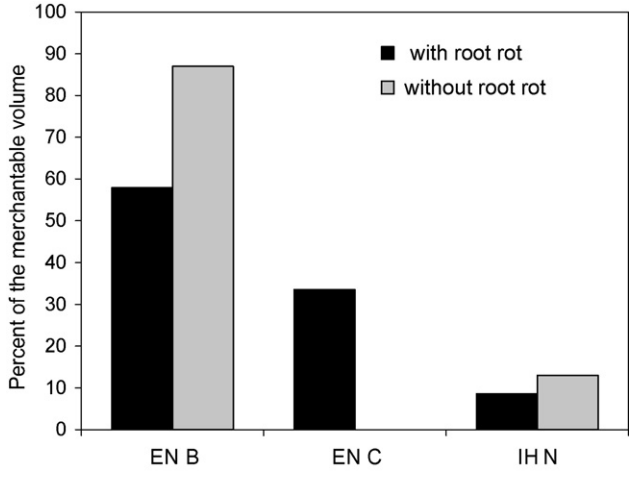

Fig. 12. Comparison of the assortment structure of a simulated stand when red rot is taken into account or when it is neglected.

5. Discussion

The rot simulation with RAM predicted plausible decay dimensions which were within the typical magnitudes published by several authors in Germany (Kató, 1967; Werner, 1971; Rehfuess, 1969; von Pechmann et al., 1973).

The two defined phases of tree–pathogen interaction were reflected in a plausible way. The results of the simulations proved that a spatial description of the rot arising in the stem is possible. This includes the prediction of the spatial extent of rot from differing degrees of decay, which is a novelty. The interaction of tree and pathogen are simulated in both directions. The tree–pathogen direction is the regulation of decay by the tree's sapwood simulated with an empirically determined maximal rot diameter. The pathogen–tree direction is the feedback on tree diameter and height growth which showed plausible results compared to literature. We can assume that only part of the growth reduction can be attributed directly to defence costs in reality, a big part may be due to opportunity costs. The infected tree cannot cope with non-infected competitors because growth is decreased. These processes are reflected very well in the scenario simulation. Nonetheless, the predicted diameter and height depression was lower than the publications of Bendz-Hellgren and Stenlid (1995, 1997) anticipate. Because the models were directly derived from their published data some inherent interactions in the growth model at the stand level or differences in the forest management can be the reason for the difference.

As there are some models for decay management developed in Scandinavia, it makes sense to compare the most recent one, published by Pukkala et al. (2005) to the proposed approach of this study. Our model RAM is limited to Norway spruce, while Pukkala et al. (2005) also predict infection and decay for Scots pine. Another difference to that approach is that Pukkala et al. (2005) distinguished between several species of *Heterobasidion* which are not accounted for in RAM.

The model of Pukkala et al. (2005) puts a focus on the epidemiological aspect of the spread from tree to tree. The approach for the simulation of decay in the stem is therefore straightforward. It is using a simple cone to describe geometric shape of the decay as a function of time since infection. In contrast, RAM models the decay expansion explicitly with regard to stem growth. This creates a feedback of stand treatment on the rot development in the stem on the single tree level. For example, if the cone model of Pukkala et al. (2005) was applied to the stem time series shown in Fig. 8 the predicted rot height and diameter would have been clearly different to the prediction of RAM (Fig. 13). The tree stem was invaded at an age of 65; a stochastic modulation of rot height like proposed by Pukkala et al. (2005) is neglected for this comparison.

The model of Pukkala et al. (2005) superimposed in broken lines over the RAM results predicts always the same conical shape which is first estimating bigger, later in the tree

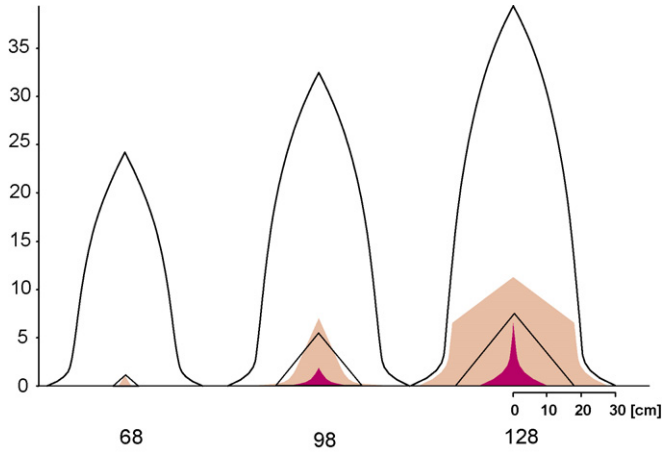

Fig. 13. Rot extent in the stem: decay predicted by RAM sensitive to stem form (grey) and superimposed the conical model of Pukkala et al. (2005) drawn as a black line.

development smaller decay proportions in the stem. The results presented here can be seen as a major refinement of the approach of Pukkala et al. (2005) considering the form of the decay column and the differentiation in different decay levels. There are also some pronounced differences in the theoretical foundations of the models. Pukkala et al. (2005) assume that the sapwood is no barrier for the fungus and their model predicts a growth reduction of the tree when the rot diameter exceeds the heartwood diameter. When the rot exceeds the stem diameter the tree ceases growth and the tree will eventually die. In contrast, the model RAM assumes the sapwood to be a barrier. For this reason the rot expansion rate is markedly reduced when the sapwood is reached. The idea behind is more a constant equilibrium of fungus and tree where none of the two is able to prevail. However, simulation runs with RAM show that infected trees die because of growth reduction due to the fungus or with other words they die if the increased opportunity costs decrease the competitiveness too much. So the fact that a very high inoculum load can lead to tree death is reflected by the model indirectly over the growth simulators competition and mortality models.

Even if there is no explicit sapwood model integrated in RAM, the maximum rot diameter predicted from RRA is taken as a substitute. As the RRA can be preset by the user for a specific stand, an adaptation of the model to specific site conditions is possible.

There is also another difference between the two models. While Pukkala et al. (2005) predict the growth reduction of the infected tree with a linear model; this work proposes a non-linear progressive depression.

However RAM is only restricted to Norway spruce and does not distinguish between different pathogens like *Heterobasidion parviporum* or *Heterobasidion abietinum* which are at present considered as separate species, and which may vary distinctly in the decay behaviour and extent. It is likely that lot of the data forming the model data base was carried out on trees infected with these species. The species-specific differences in decay are not well known up to now, but may be distinct. Furthermore RAM is only parameterised for a rot entering the tree over the roots. It does not adequately cover wound rot and is not able to predict other facultative pathogens like *Armillaria spec.*, *Resinicium bicolor* (Alb. et Schw. ex Fr.) Parmasto or *Stereum sanguinolentum* (Alb. et Schw. ex Fr.) Fr. These specialised saprotrophs are no pathogens in sensu stricto but can as well cause decay of wood. Therefore, that topic is still in need of further research.

Although the models are based on a vast number of trees, only average values of stands were available for modelling. Consequently, the true variance of the rot dimension within a stand is concealed. As a stochastic component was added in the initial assignation of RRA to each tree of the stand, some of the natural variance was eventually re-introduced into the system, however, this has to be checked in future against empirical data at tree level.

The further model developments should put a strong focus on model evaluation. A link between the ocular estimated degree of decay in the field and the real loss of wood density has to be established in the future. An appropriate method for this is computer tomography (zu Castell et al., 2005).

Furthermore information on tree–pathogen interaction should be consolidated. Revealing the processes behind growth and defence of trees could help to understand the interaction and to model the results quantitatively (Matyssek et al., 2005). Data on the influence of red rot on tree growth is needed for central European conditions. Also the integration of the changes in stem form due to decay still has to be done in the future. Several authors provide information on that topic (Henriksen and Jørgensen, 1952; Arvidson, 1954; Bendz-Hellgren and Stenlid, 1997). Including more physiological parameters like the sapwood content of trees like proposed by Pukkala et al. (2005) or the site dependent approach proposed by Seifert et al. (in press) would be an advantage as well as a model parameterisation for wound rot. The integration of wound rot would involve several new models because the assumption of a radial decay development from the pith outwards is usually not valid for decay originating from wound infection. New pathogen and tree species should be integrated in the future. Especially their integration in the epidemiological model RIM will be important to predict realistic tree infection in mixed stands.

To sum up, the proposed framework of a growth simulator, a model for the prediction of infection and a model for the prediction of decay expansion is able to transform the expertise gathered in decades of research in an operational simulation tool. It has the potential to provide the user with quantitative information of the tree growth and the pathogen development. With the help of scenario simulation the perspective of the forest manager is shifted from a static view to a perspective where he can account for the processes in the stand which alter the situation over time. Management options like thinning or grading can be chosen more target-oriented if such a decision tool is at one's hand for decision support.

6. Conclusion

The presented model, RAM, is able to simulate the extent of decay in stems of Norway spruce and can be used to provide

valuable information on the interaction of tree growth and decay development for central European conditions. RAM predicts the severity of decay and provides the necessary input data for a virtual grading for stands affected by *H. annosum*. This is an essential feature for the economically determination of harvest time. Additionally, the model offers input data for other simulation models which predict the mechanical stability of the tree or simulate different sawing patterns.

The proposed model RAM is designed to be used in combination with a single tree growth simulator and an epidemiologic model for the spread of the fungus in the stand. In this scope the framework of models can be utilized as a comprehensive decision support tool. This enables forest practitioners to develop adaptive management concepts for their specific situation and economic objectives and successfully takes into account the tree–pathogen processes in forest management.

Acknowledgements

The author gratefully acknowledges the financial support of the German Research Foundation DFG, within the framework of the collaborative research centre ''Growth and Parasite Defence'' SFB 607, as well as the financial support from the Bavarian State Forest Service in the frame of the projects V 40 and X 33 provided by the curatorship of the Bavarian Research Station for Wood and Forestry (LWF). I also want to thank Dr. Sonja Vospernik, Stefan Seifert and three anonymous reviewers for valuable comments on the text and Dan Morowitz for language revision.

References

Arvidson, B., 1954. En studie av granrotrötans (*Polyporus annosus* FR) ekonomiska kensekvendser—a study of the economic effects of root rot (*Polyporus annosus* FR.) in the Norway Spruce. Svenska Skogsvårdsföreningens Tidskift 52, 381–412.

Asiegbu, F.O., Johansson, M., Woodward, S., Hüttermann, A., 1998. In: Woodward, S., Stenlid, J., Karjalainen, R., Hüttermann, A. (Eds.), *Heterobasidion annosum*—Biology, Ecology, Impact and Control. CAB International, Wallingford, UK, pp. 167–193.

Bazzigher, G., 1986. Infection studies with *Heterobasidion annosum* on young trees of *Picea abies*. Eur. J. Forest Pathol. 16, 125–128.

Bazzigher, G., Schmid, P., 1969. Sturmschaden und Fäule. Schweizerische Zeitschrift für Forstwesen 120, 521–535.

Bendz-Hellgren, M., Stenlid, J., 1995. Long-term reduction in the diameter growth of butt rot affected Norway spruce, *Picea abies*. Forest Ecol. Manag. 74, 239–243.

Bendz-Hellgren, M., Stenlid, J., 1997. Decreased volume growth of *Picea abies* in response to *Heterobasidion annosum* infection. Can. J. Forest Res. 27, 1519–1524.

Binder, B., 1995. Grundlagen zur Bewertung von Schälschäden. Dissertation at the Institute Forest Growth Research. University of Agricultural and Applied Life Sciences (BOKU), p. 135.

Courtois, H., 1970. Einfluß von Rohdichte, Holzfeuchtigkeit und Jahrringbreite auf den Abbau des Nadelholzes durch Fomes annosus (FR.) CKE. Holz als Roh- und Werkstoff 28 (2), 67–75.

Cwielong, P., Lettojärvi, T., Hüttermann, A., 1993. Die Bedeutung des Sauerstoffs für die Physiologie von *Heterobasidion annosum*, dem Erreger der Rotfäule. Allgemeine Forst- und Jagdzeitung 164 (11), 199–203.

Dimitri, L., 1980. Untersuchungen über die Widerstandsfähigkeit der Fichte (*Picea abies* KARST.) gegenüber dem Wurzelschwamm *Fomes annosus* (FR.) COOKE. Schriften aus der Forstlichen Versuchsanstalt Göttingen und der Niedersächsischen Forstlichen Versuchsanstalt 66, 1–126.

Dimitri, L., Tomiczek, C., 1998. Germany and Austria. In: Woodward, S., Stenlid, J., Karjalainen, R., Hüttermann, A. (Eds.), *Heterobasidion annosum*—Biology, Ecology, Impact and Control. CAB International, Wallingford, UK, pp. 355–368.

Frankel, S.J., Eav, B.B., Kliejunas, J.T., Shaw III, C.G., 1994. Modelling the dynamics and impact of Annosus root rot disease in western North America. In: Johansson, M., Stenlid, J. (Eds.), Proceedings of the Eighth International Conference on Root and Butt Rots, IUFRO Working Party S2.06.01, Uppsala, Sweden, 1993, pp. 762–770.

Graber, D., 1996. Die Kernfäule an Fichte (*Picea abies* KARST.) in der Schweiz nördlich der Alpen: Untersuchungen über das Schadausmass, die ökologischen und mykologischen Einflussfaktoren sowie die ökonomischen Auswirkungen. Beiheft zur Schweizerischen Zeitschrift für Forstwesen 79, 283.

Haars, A., Chet, I., und Hüttermann, A., 1981. Effect of phenolic compounds and tannin on growth and laccase activity of *Fomes annosus*. Eur. J. Forest Pathol. 11, 67–76.

Henriksen, H.A., Jørgensen, E., 1952. Rodfordaerverangreb i relation til udhugningsgrad [*Fomes annosus* attack in relation to grade of thinning] (Danish with English abstract). Det Forstlige Forsøgsvæsen i Danmark 21, 215–252.

Hüttermann, A., Woodward, S., 1998. Historical aspects. In: Woodward, S., Stenlid, J., Karjalainen, R., Hüttermann, A. (Eds.), *Heterobasidion annosum*: Biology, Ecology, Impact and Control, A. CAB International, Wallingford, UK, pp. 1–25.

Isomäki, A., Kallio, T., 1974. Consequences of injury caused by timber harvesting machines on the growth and decay of spruce (*Picea abies* [L.] KARST.). Acta Forestalia Fennica 136, 1–25.

Johann, K., 1988. Ergebnisse einer Rotfäuleuntersuchung in sehr wüchsigen Fichtenbeständen. FBVA-Berichte—Schriftenreihe der Forstlichen Bundesversuchsanstalt Wien, vol. 25, 80 pp.

Kallio, T., Tamminen, P., 1974. Decay of spruce (*Picea abies* (L.) KARST.) in the Åland islands. Acta Forestalia Fennica 138, 1–42.

Kató, F., 1967. Beitrag zur Beurteilung einzelner schwerwiegender Probleme der Fichtenrotfäule. Forstwissen schaftliches Centralblatt 6, 348–369.

Kató, F., 1969. Stammfäuleschäden der Fichte—Ein Beitrag zur Schadensberechnung in den staatlichen Fichtenwäldern Niedersachsens mit besonderer Berücksichtigung der Schälschäden des Rotwildes. Forstarchiv 40, 81–92.

Kublin, E., Scharnagl, G., 1988. Verfahrens und Programmbeschreibung zum BWI-Unterprogramm BDAT. Forstliche Versuchs- und Forschungsanstalt Baden-Württemberg, Freiburg, p. 87.

Matyssek, R., Agerer, R., Ernst, D., Munch, J.-C., Oßwald, W., Pretzsch, H., Priesack, E., Schnyder, H., Treutter, D., 2005. The plants capacity in regulating resource demand. Plant Biol. 7, 560–580.

Möykkynen, T., Miina, J., Pukkala, T., von Weissenberg, K., 1998. Modelling the spread of butt rot in a *Picea abies* stand in Finland to evaluate the profitability of stump protection against *Heterobasidion annosum*. Forest Ecol. Manag. 106, 247–257.

Möykkynen, T., Miina, J., Pukkala, T., 2000. Optimizing the management of a *Picea abies* stand under risk of butt rot. Eur. J. Forest Pathol. 30, 65–76.

Müller, F., 2002. Modellierung von Sturm-, Schnee- und Rotfäulerisiko auf Einzelbaumebene. Dissertation, Science Center Weihenstephan of the Technische Universität München. 175 pp.

Pratt, J.E., 1979. Butt rot of sitka spruce I. Observations on the development of butt-rot in individual trees and in stands. Forestry 52 (1), 11–29.

Pratt, J.E., Shaw III, C.G., Vollbrecht, G., 1998. Modelling disease development in forest stands. In: Woodward, S., Stenlid, J., Karjalainen, R., Hüttermann, A. (Eds.), *Heterobasidion annosum*—Biology, Ecology, Impact and Control, A. CAB International, Wallingford, UK, pp. 213–233.

Pretzsch, H., 2002. Application and evaluation of the growth simulator SILVA 2.2 for forest stands, forest estates and large regions. Forstwissenschaftliches Centralblatt 121 (Suppl. 1), 28–51.

Pretzsch, H., Biber, P., Dursky, J., 2002a. The single tree-based stand simulator SILVA: construction, application and evaluation. Forest Ecol. Manag. 162, 3–21.

Pretzsch, H., Biber, P., Dursky, J., Von Gadow, K., Hasenauer, H., Kändler, G., Kenk, G., Kublin, E., Nagel, J., Pukkala, T., Skovsgaard, J.G., Sodtke, R., Sterba, H., 2002b. Recommendations for standardized documentation and further development of forest growth simulators. Forstwissenschaftliches Centralblatt 121, 138–151.

Pukkala, T., Möykkynen, T., Thor, M., Rönnberg, J., Stenlid, J., 2005. Modeling infection and spread of *Heterobasidion annosum* in even-aged Fennoscandian conifer stands. Can. J. Forest Res. 35, 74–84.

Rehfuess, K.E., 1969. Ernährungszustand und Kernfäulebefall älterer Fichtenbestände auf der Schwäbischen Alb. Mitteilungen des Vereins für Forstliche Standortskunde und Forstpflanzenzüchtung 19, 6–18.

Rehfuess, K.E., 1973. Kernfäulebefall und Ernährungszustand älterer Fichtenbestände (*Picea abies* KARST.) im Wuchsgebiet ''Baar-Wutach'' Mitteilungen des Vereins für Forstliche Standortskunde und Forstpflanzenzüchtung 22, 9–26.

Rieger, S., 1991. Untersuchungen zur Phasendisposition der Fichte (*Picea abies* (L.) KARST.) gegenüber *Heterobasidion annosum* (FR.) BREF. Dissertation an der Forstwissenschaftlichen Fakultät der Ludwig-Maximilians-Universität München, 151 pp.

Schumacher, P., Ritter, U., Schulz, H., Wegener, G., 1997. Qualitätssortierung von Fichtenstammholz nach dem Europäischen Normentwurf prEN 1927-1 (1). Holz-Zentralblatt 74, 1137–1138.

Seifert, T., 2003. Integration von Holzqualität und Holzsortierung in behandlungssensitive Waldwachstumsmodelle. Dissertation, Science Center of the Technische Universität München, 314 pp.

Seifert, T., Fürst, C., Seifert S., Knoke, T. Improving red rot and red heart prediction by modeling sapwood in Norway spruce and European beech. Proceedings of the Fifth workshop of the IUFRO working party 5.01.04 on ''Wood Quality Modelling''. Waiheke, New Zealand, in press.

Shain, L., 1971. The response of sapwood of Norway spruce to infection by *Fomes annosus*. Phytopathology 61, 301–307.

Stenlid, J., Redfern, D.B., 1998. Spread within the tree and stand. In: Woodward, S., Stenlid, J., Karjalainen, R., Hüttermann, A. (Eds.), *Heterobasidion annosum*—Biology, Ecology, Impact and Control. CAB International Wallingford, UK, pp. 125–141.

Steyrer, G., Tomiczek, C., 1998. Höhere Sturmschadensgefahr durch Wurzelfäule. Österreichische Forstzeitung 109 (4), 19.

Vollbrecht, G., Jørgensen, B.B., 1995. Modelling the incidence of butt rot in plantations of *Picea abies* in Denmark. Can. J. Forest Res. 25, 1887–1896.

von Pechmann, H., von Aufsess, H., 1971. Untersuchungen über die Erreger von Stammfäulen in Fichtenbeständen. Forstwissenschaftliches Centralblatt 90, 259–284.

von Pechmann, H., von Aufsess, H., Rehfuess, K.-E., 1973. Ursachen und Ausmaß von Stammfäulen in Fichtenbeständen auf verschiedenen Standorten. Forstwissenschaftliches Centralblatt 92, 68–89.

von Weissenberg, K., 1998. Resistance of *Picea abies* to *Heterobasidion annosum*. In: Proceedings of the Fifth International Conference on Problems of Root and Butt Rot in Conifers of the IUFRO Working Party S2.06.01, August 7–12, Kassel, Germany, pp. 67–74.

Wipfler, P., Seifert, T., Heerdt, C., Werner, H., Pretzsch, H., 2005. Growth of adult Norway spruce (*Picea abies* [L.] Karst.) and European beech (*Fagus sylvatica* L.) under free-air ozone fumigation. Plant Biol. 7, 611–618.

Werner, H., 1971. Untersuchungen über die Einflüsse des Standorts und der Bestandesverhältnisse auf die Rotfäule (Kernfäule) in Fichtenbeständen der Mittleren Alb. Mitteilungen des Vereins für Forstliche Standortskunde und Forstpflanzenzüchtung 20, 9–49.

Woodward, S., Stenlid, J., Karjalainen, R., Hüttermann, A. (Eds.), 1998. *Heterobasidion annosum*—Biology, Ecology, Impact and Control. CAB International, Wallingford, UK, p. 589.

Woodward, S., Pratt, J.E., Pukkala, T., Spanos, K.A., Nicolotti, G., Tomiczek, C., Stenlid, J., Marçais, B., Lakomy, P., 2003. MOHIEF: Modelling of *Heterobasidion annosum* in European forests, a EU-funded research program. In: LaFlamme, G., Bérubé, J., Bussières, G. (Eds.). Root and Butt Rot of Forest Trees—Proceedings of the IUFRO Working Party 7.02.01, Quebec City, Canada, September 16–22, 2001. Canadian Forest Service, Information Report LAU-X-126, 423-427.

zu Castell, W., Schrödl, S., Seifert, T., 2005. Volume interpolation of CT images from tree trunks. Plant Biol. 7, 737–744.

Zycha, H., 1962. Hymenomycetes. In: Sorauer, P., Appel, O., Blunck, H., Rademacher, B., Richter, H. (Eds.), Handbuch der Pflanzenkrankheiten. Parey-Verlag, Berlin, pp. 550–575.

Zycha, H., 1967a. Die Beurteilung des Rotfäulebefalls in Fichtenbeständen. In: Zycha, H. and Kató, F. (Eds.). Untersuchungen über die Rotfäule der Fichte. Schriftenreihe der Forstlichen Fakultät der Universität Göttingen, vol. 39, pp. 1–31.

Zycha, H., 1967b. Die Rotfäule der Fichte. In: Zycha, H., Ahrberg, H., Courtois, H., Dimitri, L., Liese, W., Peek, R.-D., Rehfuess, K.E., Schlenker, G., von Schnurbein, U., Schwantes, H.O. (Eds.). 1976: Der Wurzelschwamm (*Fomes annosus*) und die Rotfäule der Fichte (*Picea abies*). Supplement of the Forstwissenschaftliches Centralblatt, vol. 36, pp. 6–13.

Zycha, H., Dimitri, L., 1968. Ausmaß und Ursache der Kernfäule in einer Fichtenprobefläche in Reinhausen (Niedersachsen). Forstwissenschaftliches Centralblatt 87, 331–341.

Zycha, H., Ulrich, B., 1969. Die Rotfäule der Fichte. Forstarchiv 40 (11), 209–212.

Zycha, H., Dimitri, L., und Kliefoth, R., 1970. Ergebnis objektiver Messungen der durch *Fomes annosus* verursachten Rotfäule in Fichtenbeständen. Allgemeine Forst- und Jagdzeitung 141 (4), 66–73.